PERGAMON

Chemical Engineering Science 57 (2002) 2047–2058

Chemical Engineering Science

www.elsevier.com/locate/ces

Desulphurization of SO_2–N_2 mixtures by limestone slurries

R. V. Bravo[a,*], R. F. Camacho[a], V. M. Moya[b], L. A. I. García[a]

[a] *Departamento de Ingeniería Química, Facultad de Ciencias, Universidad de Granada, C/Avenida Fuentenueva s/n, 18071 Granada, Spain*
[b] *Departamento de Ingeniería Química, Ambiental y de los Materiales, Facultad de Ciencias Experimentales, Universidad de Jaén, Paraje las Lagunillas s/n, 23071 Jaén, Spain*

Received 29 March 2001; accepted 5 March 2002

Abstract

We studied the absorption of SO_2 from mixtures with N_2 into limestone slurries. The reactor used was a stirred tank with an almost flat gas–liquid interface of area 67.7×10^{-4} m^2 at 400 rpm, operated in gas-phase continuous operation mode and batchwise for the slurry. The operating temperatures used were 20°C and 40°C, the content of limestone in the initial slurry was 1, 3 and 5 wt% and the volume fraction of SO_2in the gas mixture at the inlet to the reactor ranged from 4% to 10%.

We determined the overall gas-side SO_2 transfer coefficient, obtaining values of 0.104 and 0.083 mol/s/m^2/bar at 20°C and 40°C, respectively. By taking into account the individual gas-side SO_2 transfer coefficient and estimating the enhancement factor, we were able to determine the thickness of the interfacial liquid film, 45 and 58 μm at temperatures of 20°C and 40°C, respectively, and the SO_2 physical absorption coefficient, 3.27×10^{-5} and 4.01×10^{-5} m/s at 20°C and 40°C, respectively. The results obtained are comparable with those reported in previous studies, both by ourselves and by other authors.

Keywords: Absorption; Gases; Interface; Mass transfer; Pollution; Slurries

1. Introduction

Emissions of sulphur dioxide into the atmosphere have increased steadily with industrial development. The combustion of coal, due to its high sulphur content, means it is necessary to dedicate particular attention to eliminating the resulting emissions of sulphur oxides. Among the many procedures employed to desulphurize exhaust gases, absorption into limestone slurries is the most commonly applied method due to its high degree of SO_2 absorption, low cost and widespread availability.

Pasiuk-Bronikowska, Ziajka, and Bronikowski (1992) reported the existence of various factors that favour the use of limestone slurries in the desulphurization of gas streams. The most important of these are:

(a) The need to remove SO_2 from large streams of industrial waste gases at low cost. Limestone and dolomite are abundant minerals and can easily be used in slurries with absorbent properties.
(b) The possibility of transforming the SO_2 into gypsum, a product that is both stable and reusable.
(c) The specific properties of the aqueous slurries produced by a reagent obtained by the partial dissolution of the particles in suspension; when such particles are of the appropriate diameter, shape and composition they facilitate an increase in the absorption rate.

The reactions and physical steps that may affect the absorption rate within a limestone slurry are as follows (Uchida, Moriguchi, Maejima, Koide, & Kageyama, 1978):

(1) The diffusion of SO_2 through the gas film near the gas–liquid interface.
(2) The dissolution of SO_2 in the liquid phase.
(3) The first dissociation of SO_2.
(4) The second dissociation of SO_2.
(5) The dissolution of $CaCO_3$.
(6) The diffusion of SO_2 and the different ions towards the reaction area of the liquid film.

When the partial pressure of the SO_2 is low, as normally occurs in the gases to be treated, step 1 may meet significant resistance, its strength largely depending on the operating conditions and the type of equipment used to obtain contact between the phases. Steps 2–4, which correspond to the absorption and dissociation of the SO_2, are virtually instantaneous. Step 5 corresponds to the dissolution of the $CaCO_3$

* Corresponding author. Tel.: +34-958-243310; fax: +34-9-582-48992.
E-mail address: vbravo@goliat.ugr.es (R. V. Bravo).

0009-2509/02/$ - see front matter
PII: S0009-2509(02)00095-7

in the liquid phase and is greatly affected by the concentration of the different ions and compounds present, as well as by the partial pressure of the SO_2, the particle size distribution of the limestone and the pH of the medium (Sada, Kumazawa, & Lee, 1984; Uchida & Ariga, 1985). Step 6 corresponds to the diffusion of the different species towards the area where the overall reaction is taking place:

$$CaCO_3 + SO_2 \xrightarrow{H_2O} CaSO_3 + CO_2$$

and as the calcium sulphite is highly insoluble it tends to precipitate as $CaSO_3 \cdot 1/2H_2O$. Similarly, sulphate is formed from the oxidation of sulphite and, depending on the relative concentration of each, will precipitate either jointly or separately. Pasiuk-Bronikowska et al. (1992) and Olausson, Wallin, and Bjerle (1993) reported that when the pH is below 3, $Ca(HSO_3)_2$ rather than calcium sulphite is precipitated.

The operating temperature has little influence on the kinetics of the overall process, and thus the process may be limited by the physical steps of the diffusion or dissolution of the $CaCO_3$ (Uchida et al., 1978). Furthermore, it has been shown that the absorption rate increases with the surface area of the particles, with the concentration of solids in suspension and, when a stirred tank is used, with the stirring speed of the slurry. All this underlines the fact that the dissolution rate of the $CaCO_3$ could play an important role in the overall kinetics. However, when the contact device used produces a short interfacial contact time, the absorption rate does not seem to be affected by the dissolution rate of the solid particles (Bjerle, Bengtsson, & Farnkvist, 1972).

Pasiuk-Bronikowska et al. (1992) reported that when the concentration of sulphur dioxide is less than 0.2% in volume and the absorbent used is alkaline, the main resistance to mass transfer occurs within the gas phase. When the concentration of sulphur dioxide is greater than 0.2% in volume, the liquid-side resistance to mass transfer should be taken into account.

Olausson et al. (1993) developed a model for the removal of SO_2 from flue gas by absorption into a limestone slurry within a desulphurization unit comprising an absorber tower and an oxidation tank. The absorption rates of SO_2 and CO_2 in the tower were calculated according to the two-film model. Particle size had a slight effect on the absorption capacity of the SO_2 in the scrubber unit; smaller particles dissolved faster than larger ones and so removal of SO_2 is greater when the particles of $CaCO_3$ in suspension are smaller.

Brogren and Karlsson (1997) developed a model based on the penetration theory to calculate the dynamic absorption rate of sulphur dioxide into a droplet of limestone slurry. The calculations show that the absorption of SO_2 into a limestone spray scrubber to a large extent is liquid-side controlled. Only at the very top of the absorber, where the partial pressure of SO_2 is low, is the gas film resistance above 50%. Limestone dissolution close to the gas–liquid interface has been shown to be of significance at low pH and in the parts of the absorber where the internal circulation inside the droplets is low.

Lancia, Musmarra, and Pepe (1997) carried out SO_2 absorption experiments using a bubbling reactor with a mixture of SO_2 and N_2 in the gas phase and aqueous limestone suspensions in the liquid phase. Their model, based on the film theory, was proposed to describe liquid-side mass transfer and to evaluate the enhancement factor. It was assumed that the liquid-side resistance to diffusion is concentrated within a film, the thickness of which depends on fluid dynamics conditions.

We wished to determine the applicability of modelling SO_2 absorption into $CaCO_3$ suspensions by examining the transference of the SO_2 from the gas bulk to that of the slurry and by taking into account instantaneous reactions between ions. This was done by making an experimental study of SO_2 absorption using a reactor that provided a limited contact time between the gas and the slurry, in order to avoid the influence of the dissolution rate of solid particles. The model developed by Lancia et al. (1997), which applied the film theory, has been extended to consider the case when the desorption of CO_2 may also be taken into account; thus, it is not assumed to be a negligible step.

2. Materials and methods

The experimental setup has been described in a previous paper (Bravo, Camacho, Moya, & García, 2000). The reactor used was a stirred tank with a capacity of 0.75×10^{-3} m^3 and a virtually flat gas–liquid interface of area 67.7×10^{-4} m^2 at 400 rpm (Bravo et al., 2000), operated continuously in the gas phase and batchwise for the slurry. All experiments were performed with a dry gas mixing stream of 1.667×10^{-5} m^3/s and stirring both of the gas and of the liquid phases at a speed of 400 rpm; our aim was to obtain a virtually perfect mix both of the liquid phase (Bravo, Camacho, & Moya, 1993) and of the gas phase (Bravo et al., 2000). The following parameters were used to determine the influence of the operating variables: temperature, 20°C and 40°C; proportion of limestone in the initial slurry, 1, 3 and 5 wt%; volume fraction of SO_2 in the gas mix at the reactor inlet, 4–10%. The limestone used was obtained from Torredonjimeno (Jaén, Spain) and had a purity of over 99.6%. It was ground and sieved to separate two size fractions which were characterized by granulometric analysis using a GALI-CIS-1 device. Size distributions by number, area and volume were obtained; the median value was 4.2×10^{-6} m (fraction A) and 6.2×10^{-6} m (fraction B), and the geometric standard deviations were 1.71 and 1.82, respectively.

During the absorption, and at 10-min intervals, two samples were obtained simultaneously from the slurry, in order to determine the total amount of SO_2 absorbed and the total solids: $CaCO_3$ and $CaSO_3$. We assumed, in agreement with Pasiuk-Bronikowska et al. (1992) and Olausson et al.

(1993), that $CaSO_3$ is indeed the solid precipitated, as at all times and in all the experiments,while there was $CaCO_3$ in suspension the pH of the solution was greater than 3.

The first sample was collected directly on I_2 in an acid medium and the total amount of SO_2 absorbed was determined by iodometric titration with $Na_2S_2O_3$. The second sample was rapidly passed through a filter of pore diameter 0.45×10^{-6} m to separate the precipitate, composed of undissolved $CaCO_3$ and $CaSO_3$. The filtrate was dried in an oven at 105°C for 24 h to determine the dry weight of the sample and therefore the total moles of solid per litre of solution, $M_{\text{sol.}}$

To transform the original data into molar compositions we determined the density via pycnometries. In obtaining the density correlation, we considered only the most significant of the species present, that is, the sum of the compositions of all the forms of dissolved SO_2(H_2SO_3, HSO_3^- and SO_3^{2-}), m_{DS}, the solid $CaSO_3$, m_{SC} and the undissolved $CaCO_3$, m_{CC}. By multiple regression we obtain the following:

$$\rho = \rho_a + 0.04324 m_{\text{DS}} + 0.10559 m_{\text{SC}} + 0.05938 m_{\text{CC}}, \quad (1)$$

where ρ_a is the water density at the working temperature.

Throughout this study, when the molality and molarity of solids in the slurry are indicated, this is just one means of describing the relation between the moles of each with respect to a kilogram of water or to a litre of solution.

In the system we describe, SO_2 is absorbed and the CO_2 derived from the dissolution of $CaCO_3$ in an acid medium is desorbed, and thus there is a change in the partial pressures of the two gases within the reactor. The total pressure of the gas, the sum of the partial pressures, is given by

$$P_S + P_N + P_C = P_R - P_V, \quad (2)$$

where the pressure within the reactor, P_R, is determined experimentally and the vapour pressure, P_V, is estimated as being that of the water at the working temperature.

The partial pressures were determined from the molar fractions of each gas within the reactor. The inlet molar flow rates of SO_2 and N_2 to the reactor, $Q_{S,\text{ inl}}$ and $Q_{N,\text{ inl}}$, were determined from the experimental values of the respective volumetric flow rates. We then calculated, as described below, the molar flow rate of SO_2 absorbed, $Q_{S,a}$, and that of CO_2 desorbed, $Q_{C,d}$, and from these values derived the molar fractions and partial pressures of the two gases within the reactor.

$$x_S = \frac{Q_{S,\text{ inl}} - Q_{S,a}}{Q_{C,d} + (Q_{S,\text{ inl}} - Q_{S,a}) + Q_{N,\text{ inl}}},$$

$$P_S = x_S(P_R - P_V), \quad (3)$$

$$x_C = \frac{Q_{C,d}}{Q_{C,d} + (Q_{S,\text{ inl}} - Q_{S,a}) + Q_{N,\text{ inl}}},$$

$$P_C = x_C(P_R - P_V). \quad (4)$$

These values coincide with the outlet values, as we assume the hypothesis of perfect mixing.

3. Results and discussion

Whatever its state of crystallization, $CaCO_3$ is highly insoluble in water, but the fraction that does dissolve does so as

$$CaCO_{3(s)} \rightarrow CO_3^{2-} + Ca^{2+} \quad (5)$$

while the ions react as follows with the water:

$$CO_3^{2-} + H_2O \leftrightarrows HCO_3^- + OH^-, \quad (6)$$

$$HCO_3^- + H_2O \leftrightarrows H_2CO_3 + OH^-, \quad (7)$$

$$Ca^{2+} + H_2O \leftrightarrows CaOH^+ + H^+ \quad (8)$$

and the reaction of the $CaOH^+$ to produce calcium hydroxide is almost imperceptible; thus the saturated solution of $CaCO_3$ is alkaline. This alkaline nature, however, is not maintained when SO_2 is absorbed, due to its higher acidity than the carbonate ion. The resulting solution, therefore, presents an acidic pH. In consequence, reaction (8) is practically absent, and so, in addition to reactions (6) and (7), the following must be taken into consideration:

$$H_2CO_3 \rightarrow CO_{2(g)} + H_2O, \quad (9)$$

$$SO_{2(g)} + H_2O \rightarrow H_2SO_3, \quad (10)$$

$$H_2SO_3 \leftrightarrows HSO_3^- + H^+, \quad (11)$$

$$HSO_3^- \leftrightarrows SO_3^{2-} + H^+, \quad (12)$$

$$Ca^{2+} + SO_3^{2-} \leftrightarrows CaSO_{3(s)}. \quad (13)$$

In order to determine the concentration of all the chemical species present in the slurry, we take into account the corresponding equilibrium constants of the reactions (6), (7), (11) and (12), the solubility product of Eq. (13) and the water autoprotolysis constant, K_W, all assumed to be instantaneous:

$$\text{Equilibrium (6)} \rightarrow K_{2C} = \frac{m_{C2} m_H}{m_{C1}} \frac{\gamma_{C2}\gamma_H}{\gamma_{C1}}, \quad (14)$$

$$\text{Equilibrium (7)} \rightarrow K_{1C} = \frac{m_{C1} m_H}{m_{C0}} \frac{\gamma_{C1}\gamma_H}{\gamma_{C0}}, \quad (15)$$

$$\text{Equilibrium (11)} \rightarrow K_{1S} = \frac{m_{S1} m_H}{m_{S0}} \frac{\gamma_{S1}\gamma_H}{\gamma_{S0}}, \quad (16)$$

$$\text{Equilibrium (12)} \rightarrow K_{2S} = \frac{m_{S2} m_H}{m_{S1}} \frac{\gamma_{S2}\gamma_H}{\gamma_{S1}}, \quad (17)$$

$$\text{Equilibrium (13)} \rightarrow K_{sp,\text{ SC}} = m_{\text{DC}} m_{S2} \gamma_{\text{DC}} \gamma_{S2}, \quad (18)$$

$$\text{Water autoprotolysis} \rightarrow K_w = m_H m_{\text{OH}} \gamma_H \gamma_{\text{OH}}. \quad (19)$$

Appendix A contains the expressions used to calculate the thermodynamic constants and the activity coefficients defined in Eqs. (14)–(19). Taking into account, furthermore, the condition of electroneutrality,

$$m_{S1} + 2m_{S2} + m_{C1} + 2m_{C2} = 2m_{DC} + m_H \tag{20}$$

the material balances,

$$\text{Calcium} \rightarrow m_{CC0} = m_{DC} + m_{CC} + m_{SC}, \tag{21}$$

$$\text{Carbon} \rightarrow m_{CC0} = m_{CC} + m_{Cd} + m_{C0} + m_{C1} + m_{C2}, \tag{22}$$

$$\text{Sulphur} \rightarrow m_{ST} = m_{S0} + m_{S1} + m_{S2} + m_{SC} \tag{23}$$

and the fact that the sum of the mass fractions of all the species within the mixture must be equal to one, it is possible to determine from the initial data (moles of limestone per kg of water in the slurry) and from the analysis (pH of the solution and mass fraction of total SO_2) the concentration of all the chemical species in the slurry and also the changes in the volume of the solution due to the absorption of SO_2, the desorption of CO_2, the precipitation of $CaSO_3$ and the dissolution of $CaCO_3$.

After considering all the variables and equations utilized, there remained one degree of freedom, which meant a new variable had to be defined. No experimental data were available for the CO_2 desorbed, so a variable, Y, is introduced to represent the ratio of the moles of CO_2 desorbed to those of dissolved $CaCO_3$

$$Y = \frac{m_{Cd}}{m_{CC0} - m_{CC}}. \tag{24}$$

Initially, this variable satisfies the above-mentioned degree of freedom, and so a prior value must be assumed that enables us to resolve the whole system of equations, although this can be calculated later, after determining the profiles of the chemical species within the liquid film.

In the liquid bulk of the reactor, operating as described above, it is verified that the accumulation of SO_2, in all the forms possible within the slurry, dn_S/dt, must equal the molar flow rate of SO_2 across the interface, this being the product of the flux, N_S, and the interface area, A.

$$\frac{dn_S}{dt} = N_S A. \tag{25}$$

To evaluate the total number of moles of SO_2 absorbed during the time interval between two consecutive samples ($\Delta t_j = t_j - t_{j-1}$) it is possible to multiply the difference in molarity by the mean solution volume, $V_{m\,j}$, that corresponds to this time interval.

$$n_{S,\,j} = (M_{ST,\,j} - M_{ST,\,j-1})V_{m,\,j}. \tag{26}$$

This enables us to determine the derivative of Eq. (25) and thus obtain the flux of SO_2 across the interface

$$N_S = \frac{1}{A}\frac{dn_S}{dt} = \frac{1}{A}\frac{d(VM_{ST})}{dt} = \frac{V_m}{A}\frac{dM_{ST}}{dt} \tag{27}$$

which is found to be constant throughout each experiment while there is undissolved $CaCO_3$. By integrating for the generic time interval, Δt_j, we obtain

$$M_{ST,\,j} - M_{ST,\,j-1} = (N_S A)\frac{\Delta t_j}{V_{m,\,j}} \tag{28}$$

which when applied to the first and successive samples obtained for analysis, enables the following equation to be deduced:

$$M_{ST,\,j} = (N_S A)\sum_{j=1}^{n_{CC}} \frac{\Delta t_j}{V_{m,\,j}}, \tag{29}$$

where n_{CC} indicates the sample obtained prior to the total dissolution of the solid $CaCO_3$ or, if it does not dissolve totally during the experimental period, the total number of samples taken.

By applying the same treatment to the CO_2 desorbed as to the total SO_2 absorbed, we obtain an expression that is analogous to Eq. (29)

$$M_{C,\,j} = (N_C A)\sum_{j=1}^{n_{CC}} \frac{\Delta t_j}{V_{m,\,j}} \tag{30}$$

and from this we can determine the flux of the CO_2, N_C, across the interface. In this case, $M_{C,\,j}$ represents at each moment the relation between the moles of CO_2 desorbed and the volume of solution.

The partial pressures of the different gases in the gas bulk, Eqs. (3) and (4), are used to calculate the composition of the species at the interface. Thus, the composition of free SO_2 and of free CO_2 at the interface is determined by means of Henry's constants for each operating temperature, as described in Appendix B. In order to apply these constants, it is first necessary to obtain the partial pressure of each gas at the interface, which is done by applying the equations for the gas-side mass transfer,

$$N_S = k^0_{g,\,S}(P_S - P_{S,\,i}), \tag{31}$$

$$N_C = k^0_{g,\,C}(P_{C,\,i} - P_C) \tag{32}$$

as the two individual gas-side mass transfer coefficients are known (the values used and how they were obtained are described in Appendix B).

When the compositions of free SO_2 and CO_2 at the interface are known, the next step is to calculate the composition of the remaining ion and molecular species. We did not use the solubility product of the $CaSO_3$, as this assumes the inexistence of solids at the interface (Pasiuk-Bronikowska & Rudzinski, 1991), but just the equilibrium constants corresponding to Eqs. (6), (7), (11) and (12) and to the water

autoprotolysis. Additionally it must be taken into consideration that the net charge transport between the gas and the liquid is zero (Lancia et al., 1997) and that the sum of the mass fractions of all the species present is equal to one. Fick's Law and the boundary conditions of the liquid film are used to integrate the expression of the net charge transport, under the condition that there is no profile for the calcium ion.

The flux of SO_2 is given by

$$N_S = k^0_{g,\,S}(P_S - P_{S,\,i}) = N_{S0} + N_{S1} + N_{S2} = K_g(P_S - P_{S,\,e}), \tag{33}$$

where K_g represents the overall gas-side SO_2 transfer coefficient and $P_{S,e}$ the partial pressure of SO_2 in equilibrium with the free SO_2 present in the liquid bulk determined by means of Henry's constant, Eq. (B.4) in Appendix B. By considering the film theory, applying Fick's Law and the boundary conditions at the interface, and then integrating, we obtain the following equation:

$$N_S = D_{S0}\frac{M_{S0,\,i} - M_{S0}}{\delta} + D_{S1}\frac{M_{S1,\,i} - M_{S1}}{\delta} + D_{S2}\frac{M_{S2,\,i} - M_{S2}}{\delta} \tag{34}$$

which enables us to determine the thickness of the interfacial liquid film, δ.

By also considering the expression for the flux of CO_2 across the interface,

$$N_C = N_{C0} + N_{C1} + N_{C2} \tag{35}$$

and considering the film theory, applying Fick's Law and the boundary conditions at the interface, and then integrating, we obtain the equation from which M_{C0} can be determined:

$$N_C = D_{C0}\frac{M_{C0} - M_{C0,i}}{\delta} + D_{C1}\frac{M_{C1} - M_{C1,i}}{\delta} + D_{C2}\frac{M_{C2} - M_{C2,i}}{\delta} \tag{36}$$

by using the value of δ calculated from Eq. (34).

After determining the composition of free CO_2 in the bulk of the liquid phase, M_{C0}, and using the material balance to carbon, Eq. (22), together with the equilibrium constants for the carbonic acid, Eqs. (14) and (15), the value of Y is calculated from Eq. (24). This variable was assumed before when calculating the concentration of all the species in the bulk of the slurry, and so it is now possible to perform a trial and error recalculation of the value until in two successive cycles the difference is within the required precision.

3.1. Variation of the chemical species concentration over time

Before studying the influence of the operating variables on absorption, it is useful to show the variation over time of some of the most significant variables determined by the above-described calculation procedure. Figs. 1–3 illustrate,

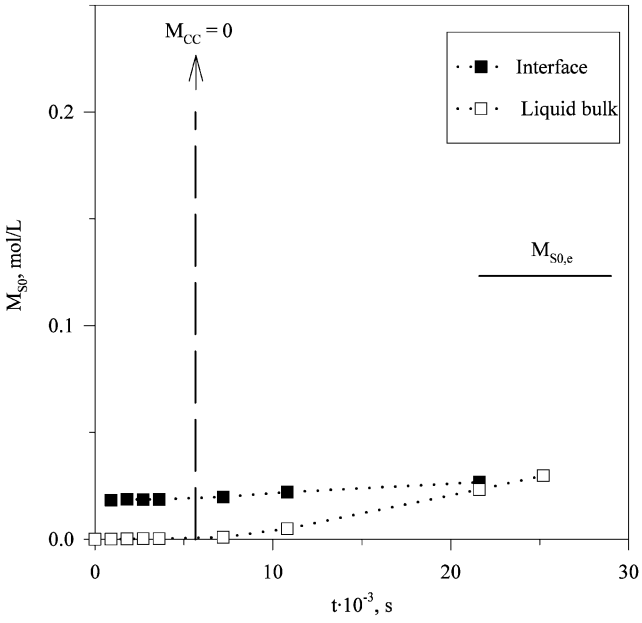

Fig. 1. The molar concentration of free SO_2 (S0) in the liquid bulk and at the interface versus the time.

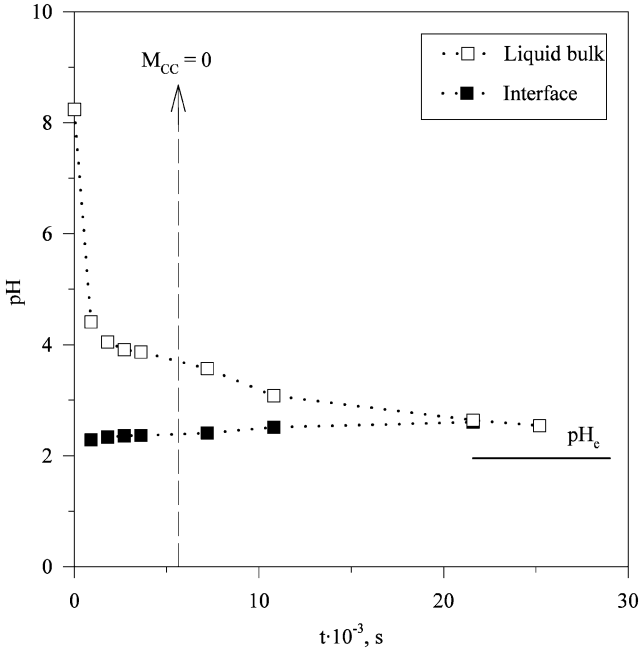

Fig. 2. Experimental pH in the liquid bulk and at the interface versus the time.

with a vertical line, the instant calculated in which total dissolution of the $CaCO_3$ occurs. The present study considers only the results obtained before this instant.

For example, Fig. 1 shows the molar concentration of free SO_2 (S0) in the liquid bulk and at the interface, together with the tendency of these two to converge to the equilibrium value for the liquid phase, estimated from the absorption in water, according to the P_S value (Camacho, Bravo, Tortosa,

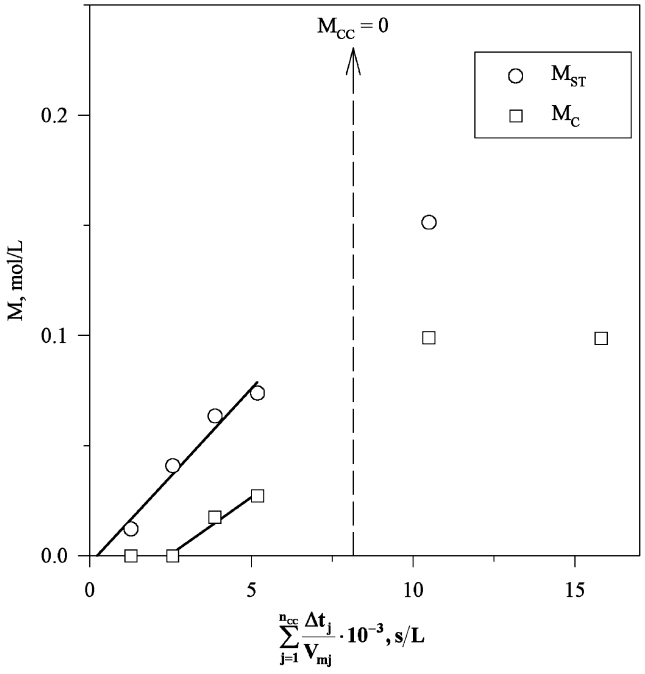

Fig. 3. Molarities of total SO_2 absorbed, M_{ST} and of CO_2 desorbed, M_C, versus the summation defined in Eqs. (29) and (30).

& Ruiz, 1986). Note that while there is undissolved $CaCO_3$, the molarity values of free SO_2 in the liquid bulk and at the interface remain almost constant, and well below the equilibrium value. The former, moreover, presents a very low value.

Fig. 2, corresponding to the same experiment, shows the experimental pH values in the bulk liquid phase, the values calculated at the interface and those corresponding to the equilibrium between phases. It can be seen that the bulk and interface values tend to converge, and that when the $CaCO_3$ is exhausted, they converge to the equilibrium value.

To determine the SO_2 flux and the CO_2 flux across the interface, N_S and N_C, Fig. 3 shows the molarities of total SO_2 absorbed, M_{ST}, and of CO_2 desorbed, M_C, versus the summation defined in Eqs. (29) and (30), for the same experiment described in Figs. 1 and 2. Fitting by least squares was used to obtain the flux as the slope of the straight lines, using only the results obtained before total dissolution of the $CaCO_3$ and, in the case of the CO_2, after its desorption has begun.

3.2. Influence of operating conditions

As remarked above, the operating conditions that were modified during the experiments were the volume percentage of SO_2 at the reactor inlet, the size and weight of the solid content in the initial slurry, and the operating temperature. Table 1 describes the experiments performed, the operating conditions applied and the rates for SO_2 absorption and CO_2 desorption determined by fitting procedures analogous to those of Fig. 3.

Fig. 4 shows all the values calculated for the total moles of solid (undissolved $CaCO_3$ and $CaSO_3$) per litre of solution, $M_{sol,\,cal}$, versus the corresponding experimental values, $M_{sol,\,exp}$. There is an acceptable degree of agreement between the experiments with the lowest initial percentage of solids in suspension, while experimental values were usually below the calculated values in the case of the highest percentages, which could be due to the fact that, depending on the operating conditions, only a part of the $CaSO_3$ is precipitated, while the rest remains in the form of $CaSO_3^0$ ion pairs.

We wished to study the influence of the operating variables on the absorption process, taking into account the possible effects of the composition of the gas phase. Fig. 5, therefore, shows, for all the experiments carried out, the N_S and N_C values divided by the partial pressure of the SO_2 at the reactor inlet plotted versus the $CaCO_3$ molarity at the start of the experiment. The figure shows that the operating temperature does not seem to have a significant influence on the rate of SO_2 absorption or of CO_2 desorption. Neither are these affected by the use of different concentrations or sizes of the initial solid. Therefore, the only factor that seems to be significant within the experimental conditions assayed (Table 1) is the SO_2 content in the gas phase.

With this in mind, we determined, for each experiment, the overall gas-side SO_2 transfer coefficient, K_g, defined in the final equality of Eq. (33). This was found to be constant and independent of the initial conditions, only being affected by the operating temperature. The values obtained were 0.104 and 0.083 mol/s/m^2/bar at 20°C and 40°C, values lower than those of the corresponding $k^0_{g,\,S}$ (Appendix B), which is indicative of how the absorption process is controlled by the transport through the two phases as the resistance of the gas phase ($1/k^0_{g,\,S}$) represents 51% at 20°C and 32% at 40°C with respect to total resistance ($1/K_g$).

Fig. 6 shows all the values for Y obtained versus experimental time. It is apparent that Y only depends on the temperature and on the time, while desorption occurs at times greater than approximately 30 min. The following correlation was obtained by nonlinear regression fitting:

$$Y = 1 - \frac{0.4\exp(2200/T)}{(t)^{0.5\exp(158/T)}} \tag{37}$$

and this was used to plot the curves for the figure.

Finally, Fig. 7 illustrates all the values of δ versus experimental time, for each temperature. The mean values for each temperature are 45 and 58 μm at 20°C and 40°C, respectively, these values agree acceptably with those at 25°C of 54 and 51 μm indicated by Sada, Kumazawa, Hashizume and Nishimura (1982) and Lancia, Musmarra, Pepe, and Volpicelli (1994). According to film theory, k^0_1 can be determined from the thickness of the interfacial liquid film:

$$k^0_1 = \frac{D_{S0}}{\delta} \tag{38}$$

Table 1
Operating conditions and flux of SO_2 and of CO_2 across the interface

T (°C)	CC0 (wt%)	Fraction	P_S, inl (bar)	$N_S \times 10^3$ (mol/s/m^2/bar)	$N_C \times 10^3$ (mol/s/m^2/bar)
20	1	B	0.0745	3.72	—
20	1	B	0.0370	2.03	1.67
20	1	A	0.0650	3.28	—
20	3	B	0.0743	3.91	3.26
20	3	B	0.0370	2.00	1.89
20	3	A	0.0648	3.20	2.86
20	3	A	0.0371	2.06	1.83
20	5	B	0.0465	2.57	2.38
20	5	B	0.0465	2.58	2.43
20	5	A	0.0744	3.68	3.20
20	5	A	0.0371	2.05	1.93
40	1	B	0.0440	2.18	1.52
40	1	A	0.0705	3.33	2.31
40	1	A	0.0439	2.35	1.53
40	3	B	0.0700	3.12	2.55
40	3	B	0.0352	1.89	1.29
40	3	A	0.0790	3.52	2.92
40	3	A	0.0352	1.71	1.63
40	5	B	0.0834	4.05	3.98
40	5	B	0.0350	1.89	1.63
40	5	A	0.0834	3.71	3.57

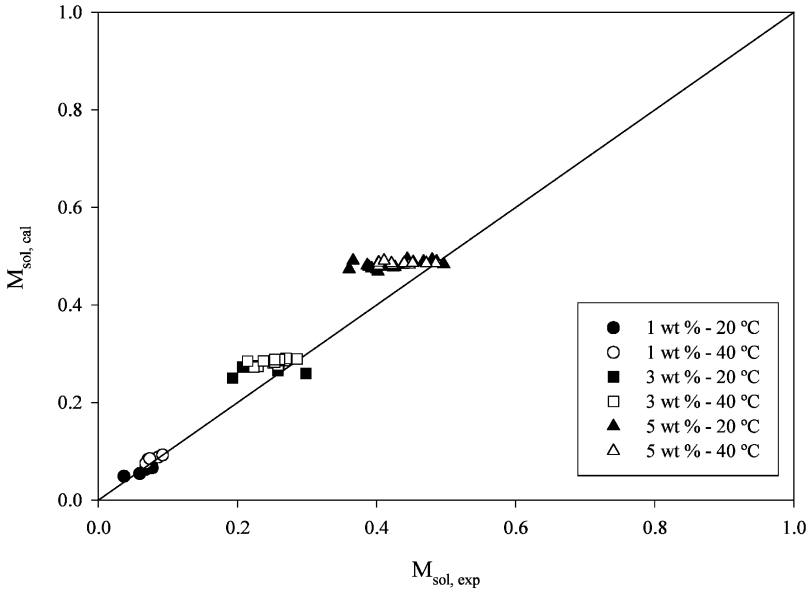

Fig. 4. Total moles of solid per litre of solution, calculated versus experimental values.

which gives values of 3.27×10^{-5} and 4.01×10^{-5} m/s at 20°C and 40°C, respectively.

To test whether the values of k_1^0 are consistent, they are plotted in Fig. 8 versus temperature values, for comparison with: (a) those corresponding to a previously established equation (Bravo, Camacho, & Moya, 1991) for SO_2 absorption in water, although it should be noted that the reactor used had a capacity of 0.25×10^{-3} m^3 and that the experiments were performed at 200 rpm rather than 400 rpm; (b) the values for k_1^0 estimated from the oxygen physical absorption coefficient in the 0.25×10^{-3} m^3 reactor but at a stirring rate of 400 rpm (Bravo, Camacho, & Moya, 1992), after transformation into values corresponding to SO_2 transfer by multiplication, according to the film theory, by the ratio of diffusion coefficients; and (c) the values determined by other authors using reactors and conditions that were analogous to those of the present study (Sada et al., 1982; Pasiuk-Bronikowska & Ziajka, 1985; Ulrich, Rochelle, & Prada, 1986; Pasiuk-Bronikowska & Rudzinski, 1991). The values obtained by these authors are in acceptable agreement

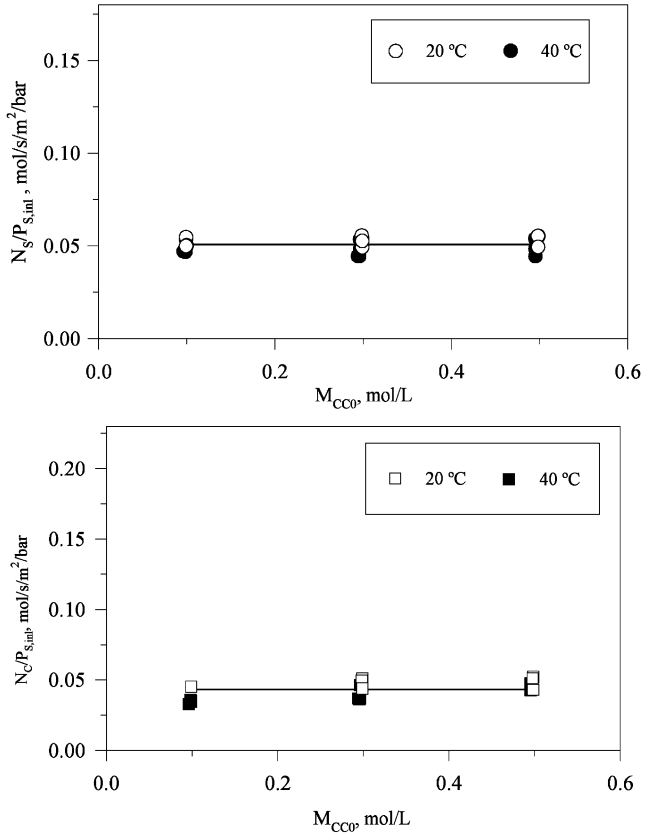

Fig. 5. Flux of SO_2 and of CO_2 divided by the partial pressure of the SO_2 at the reactor inlet versus the $CaCO_3$ molarity at the start of the experiment.

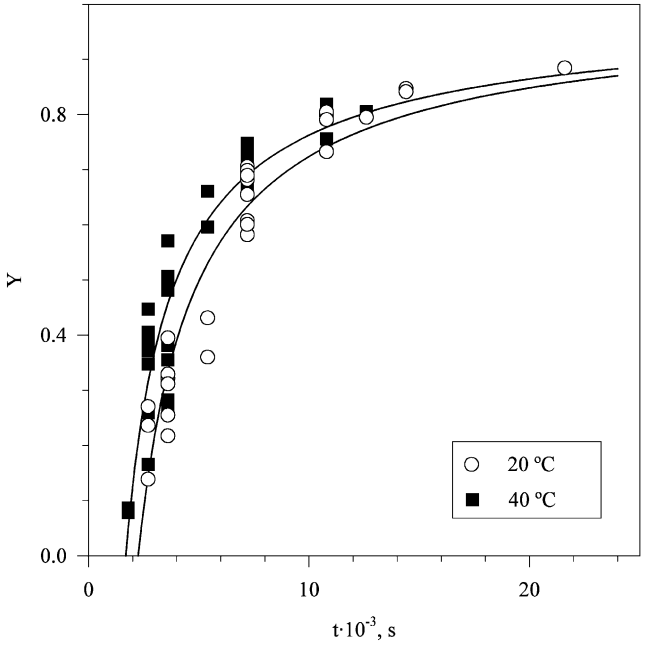

Fig. 6. Ratio of the moles of CO_2 desorbed to those of dissolved $CaCO_3$ versus the time.

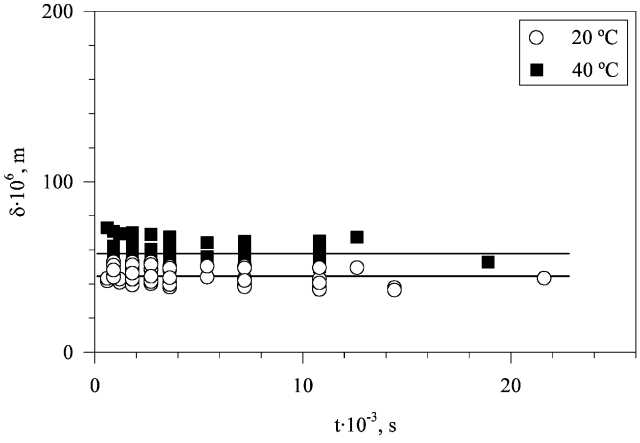

Fig. 7. Thickness of the interfacial liquid film versus the time.

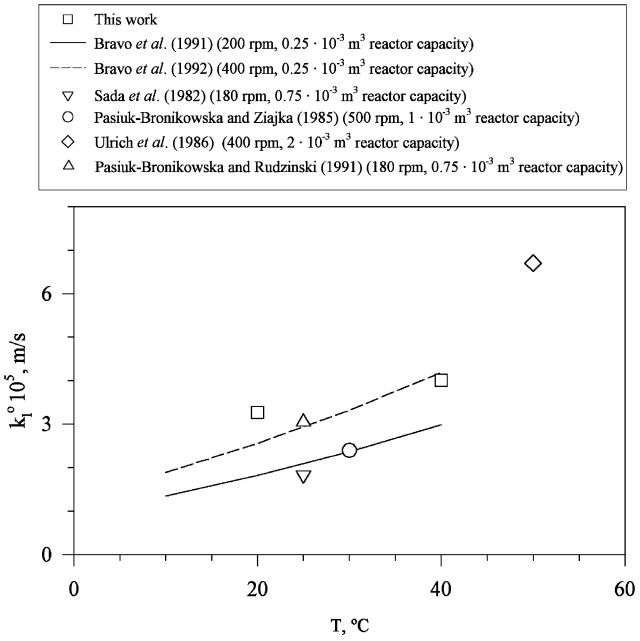

Fig. 8. SO_2 physical absorption coefficient versus the temperature.

with those established in the present study, which corroborates the hypothesis that, under the experimental conditions assayed, the limiting step of the global process of SO_2 absorption within $CaCO_3$ slurries is the SO_2 transfer through the two phases.

4. Conclusions

We have developed a calculation procedure that uses the values for the limestone content in the initial slurry, the total SO_2 in the liquid phase and the pH to determine the concentrations of all the species.

The experimental values demonstrate the considerable reduction in the absorption rate as the $CaCO_3$ disappears from the slurry, and that the flux of SO_2 across the gas–liquid

interface does not vary significantly with the operating temperature. We assume, therefore, that the reactions are instantaneous and that the process is limited by a physical step.

The flux of SO_2 across the gas–liquid interface is also practically independent of the $CaCO_3$ content by weight in the initial slurry and of the particle size of the $CaCO_3$, within the range tested, although the one assayed in this study was limited.

On the basis of the above conclusions we determined the thickness of the interfacial liquid film. Within the intervals used for the different variables being tested, the mean thickness was 45 and 58 μm at 20°C and 40°C, respectively. From these data, and using the values for the diffusion coefficient of SO_2 in the liquid phase at the above operating temperatures, we determined the SO_2 physical absorption coefficient. The values obtained were 3.27×10^{-5} and 4.01×10^{-5} m/s at 20°C and 40°C, respectively. These values are comparable to those achieved by other authors and by the present authors in previous studies of the absorption of SO_2 and of O_2.

Notation

A	interface area, m^2
K	equilibrium constants
K_g	overall gas-side SO_2 transfer coefficient, mol/s/m^2/bar
k_g^0	Individual gas-side mass transfer coefficient, mol/s/m^2/bar
k_1^0	SO_2 physical absorption coefficient, m/s
M	molarity, mol/l
m	molality, mol/kg
N	flux, mol/s/m^2
P	partial pressure, bar
Q	molar flow rates, mol/s
T	temperature, °C
t	time, s
x	molar fraction
Y	ratio of the moles of CO_2 desorbed to those of dissolved $CaCO_3$

Greek letters

ρ	density, kg/m^3
δ	thickness of the interfacial liquid film, μm
γ	molal activity coefficient

Subscripts

a	absorbed
C	CO_2
$C0$	H_2CO_3
$C1$	HCO_3^-
$C2$	CO_3^{2-}
CC	undissolved $CaCO_3$
CC0	initial $CaCO_3$
Cd	desorbed H_2CO_3
DC	Ca^{2+}
d	desorbed
e	equilibrium
H	H^+
i	interface
inl	inlet
N	N_2
0	initial
OH	OH^-
S	SO_2
$S0$	H_2SO_3
$S1$	HSO_3^-
$S2$	SO_3^{2-}
SC	solid $CaSO_3$
Sol	total solids
ST	total SO_2

Appendix A. Equilibrium constants

A.1. Thermodynamic equilibrium constants

- Eqs. (14), (15) and (19). To determine the constants of these equations, Lowell, Ottmers, Schwitzgebel, Strange, and Deberry (1970) and Olausson et al. (1993) proposed the expression:

$$\log K = -\frac{A}{T} - BT + C \tag{A.1}$$

with the parameters indicated in Table 2.

- Eq. (16)

$$K_{1S} = \exp\left[\frac{1972.5}{T} - 10.6819\right] \tag{A.2}$$

proposed by Astarita, Savage, and Bisio (1983).

- Eq. (17)

$$K_{2S} = \exp\left[\frac{1398.16}{T} - 21.288\right] \tag{A.3}$$

proposed by Hayon, Treinin, and Wilf (1972).

- Eq. (18)

$$\log K_{\mathrm{sp,SC}} = \frac{838.3}{T} - 9.7572 \tag{A.4}$$

proposed by Tseng and Rochelle (1986).

A.2. Activity coefficients

To solve Eqs. (14)–(19) it is necessary to determine the molal activity coefficients. For this purpose, we use Debye and Hückel's equation (Lowell et al., 1970):

$$-\log \gamma_i = \frac{A z_i^2 \sqrt{I}}{1 + B\mathring{a}_i \sqrt{I}}, \tag{A.5}$$

Table 2
Parameters of Eq. (A.1)

	A	B	C
K_{1C}	3404.71	0.03279	14.844
K_{2C}	2902.39	0.02379	6.498
K_w	4470.99	0.01706	6.088

Table 3
Parameters of Eq. (A.5)

T (°C)	20	40
A	0.507	0.524
B	0.328	0.331

where z_i is the valence of ion i, $\mathring{a}_i$ is the parameter of size for each ion and I is the molal ionic strength. Parameters A and B are a function of the temperature and the dielectric constant of the solvent. The values of the latter at the operating temperatures, related to the ion size (in angstroms) and utilisation of molalities, are shown in Table 3.

The values used for the ion size parameter can be seen in Table 4 (Klotz & Rosenberg, 1991).

For the molecular species, SO_2 and CO_2, the equation used to calculate the activity coefficient is the one reported by Chang and Rochelle (1982), modified to refer the coefficient to molalities

$$\gamma_0 = \frac{10^{0.076 I_M}}{c_{AG}}, \tag{A.6}$$

where c_{AG} represents the kg of water per litre of solution, and in which the value of γ_0 is assumed to be the same for all the molecular species and where the ionic strength, I_M, in mol/l, is used.

Appendix B. Calculation of thermodynamic and kinetic parameters

B.1. Gas-side mass transfer coefficients

The values of $k^0_{g,S}$ were previously determined, experimentally, by the absorption of SO_2 from mixtures of N_2 in solutions of NaOH (Bravo et al., 2000). These values were 0.204 and 0.261 mol/s/m^2/bar at 20°C and 40°C, respectively. The values of this coefficient for CO_2 transport were determined from those corresponding to SO_2 after modification, according to film theory, by the diffusivity ratio of the two gases in the gas phase.

$$k^0_{g,C} = k^0_{g,S} \frac{D_{C,g}}{D_{S,g}}. \tag{B.1}$$

This equation was applied using a ratio of 1.247 irrespective of the temperature (Reid, Prausnitz, & Sherwood, 1987) between the diffusivities of SO_2 and CO_2 in nitrogen. The values thus obtained for $k^0_{g,C}$ were 0.254 and 0.325 mol/s/m^2/bar at 20°C and 40°C, respectively.

B.2. Henry's constants

The expression for Henry's constant used for SO_2 absorption in slurries of $CaCO_3$ is a modification of the one proposed by Camacho et al. (1986) for SO_2 absorption in pure water.

$$H^0_S = \frac{m^0_{S0,i}}{P_{S,i}} = \exp\left(\frac{3100}{T} - 0.204 P_{S,i} - 10.06\right). \tag{B.2}$$

The van Krevelen and Hoftijzer equation was used to establish the saline effect on the solubility of the SO_2; this equation relates Henry's constant to the molar ionic strength by

$$\log \frac{H_S}{H^0_S} = h I_{M,i} = \log \frac{m_{S0,i}}{m^0_{S0,i}} \tag{B.3}$$

and we have considered a global value for h that represents the contribution of all the ionic species and of the gases present. After estimating the value of h for each experiment, it was observed to be proportional to the partial pressure of SO_2 at the interface. The constant of proportionality was practically the same for all experiments, which enables us to obtain the following correlation from Eqs. (B.2) and (B.3).

$$H_S = \frac{m_{S0,i}}{P_{S,i}}$$

$$= \exp\left[\frac{2712}{T} + (103.9 I_{M,i} - 16.86) P_{S,i} - 8.26\right]. \tag{B.4}$$

The values of Henry's constant for CO_2 were determined by the following equation, which is valid for the range 273–353 K.

$$\ln x_C = -159.854 + \frac{8741.68}{T}$$

$$+21.6694 \ln T - 1.10261 \times 10^{-3} T. \tag{B.5}$$

This provides the molar fraction of CO_2 in water at the pressure of 1.013 bar (Fogg & Gerrard, 1991). The values obtained for H_C, 25.96 and 42.66 bar/kg/mol at 20°C and

Table 4
Ion size parameters of Eq. (A.5)

Ions	H^+	Ca^{2+}	OH^-	HSO_3^-	SO_3^-	HCO_3^-	CO_3^{2-}
$\mathring{a}_i$,(Å)	9	6	3.5	4.5	4.5	4.5	4.5

Table 5
Values for the diffusion coefficients, $D(\times 10^9\ m^2/s)$

Species	(T (°C)) 25	20	40
SO^2	1.76	1.46	2.32
HSO_3^-	1.33	1.18	1.93
SO_3^{2-}	0.96	0.85	1.39
H^+	9.3	8.21	13.5
OH^-	5.27	4.65	7.63
CO_2	2	1.71	2.71
HCO_3^-	1.2	1.06	1.74
CO_3^{2-}	0.7	0.62	1.01
Ca^{2+}	0.79	0.7	1.14

40°C, respectively, are in reasonable agreement with those achieved by Goode and Mercer (1997).

B.3. Diffusion coefficients in the liquid phase

The diffusion coefficients of the ionic species were calculated, for the respective operating temperatures, using those proposed for water at 25°C by Chang and Rochelle (1981, 1982), Dutta, Basu, Pandit, and Rai (1987) and Lancia et al. (1997), on the assumption that for each of these the $(D\mu/T)$ ratio is constant

The diffusion coefficient of SO_2 in water was determined by the following equation:

$$D_{S0} = 5.08982 \times 10^{-12} T \times \exp\left[5.15581 - \frac{1243.06}{(T - 53.19)}\right] \frac{m^2}{s} \quad \text{(B.6)}$$

proposed by Pasiuk-Bronikowska and Rudzinski (1991) and the diffusion coefficient of CO_2 in water was calculated from the expression proposed by Versteeg, Blauwhoff, and van Swaaij (1987):

$$D_{C0} = 2.35 \times 10^{-6} \exp\left[-\frac{2119}{T}\right] \frac{m^2}{s}. \quad \text{(B.7)}$$

Table 5 gives the bibliographic values at 25°C and those used for the present calculations at 20°C and 40°C.

References

Astarita, G., Savage, D. W., & Bisio, A. (1983). *Gas treating with chemical solvents*. New York: Wiley.

Bjerle, I., Bengtsson, S., & Farnkvist, K. (1972). Absorption of SO_2 in $CaCO_3$-slurry in a laminar jet absorber. *Chemical Engineering Science*, *27*, 1853–1861.

Bravo, V., Camacho, F., & Moya, M. (1991). Absorción de SO_2 en disoluciones de citrato monosódico. *Anales Química*, *87*(3), 363–370.

Bravo, V., Camacho, F., & Moya, M. (1992). Absorción simultánea de SO_2yO_2 en agua. *Afinidad*, *IL*(437), 53–60.

Bravo, V., Camacho, F., & Moya, V. (1993). Absorción simultánea de SO_2yO_2 en disoluciones de $MnSO_4$. *Anales Química*, *89*(3), 325–331.

Bravo, V., Camacho, F., Moya, M., & García, A. I. (2000). Absorción de mezclas SO_2–N_2 en disoluciones de NaOH. *Afinidad*, *LVII*(485), 10–16.

Brogren, C., & Karlsson, H. (1997). Modeling the absorption of SO_2 in a spray scrubber using the penetration theory. *Chemical Engineering Science*, *52*(18), 3085–3099.

Camacho, F., Bravo, V., Tortosa, J., & Ruiz, J. M. (1986). Equilibrio de absorción de SO_2 en agua. *Anales Química*, *82*, 399–405.

Chang, C. S., & Rochelle, G. T. (1981). SO_2 Absorption into aqueous solutions. *A.I.Ch.E. Journal*, *27*(2), 292–298.

Chang, C. S., & Rochelle, G. T. (1982). Effect of organic acid additives on SO_2 absorption into $CaO/CaCO_3$ slurries. *A.I.Ch.E. Journal*, *28*(2), 261–266.

Dutta, B. K., Basu, R. K., Pandit, A., & Rai, P. (1987). Absorption of SO_2 in citric acid–sodium citrate buffer solutions. *Industrial & Engineering and Chemical Research*, *26*(7), 1291–1296.

Fogg, P. G. T., & Gerrard, W. (1991). A critical evaluation of gas/liquid systems in theory and practice. *Solubility of gases in liquids* (pp. 242–243). Chichester: Wiley.

Goode, S. R., & Mercer, E. E. (1997). Henry's law constants in water. The University of South Carolina. http://www.chem.sc.edu/goode/C112Web/CH12NF/sld031.htm.

Hayon, E., Treinin, A., & Wilf, J. (1972). Electronic spectra, photochemistry and autoxidation mechanism of the sulfite–bisulfite–pyrosulfite systems. *Journal of American Chemical Society*, *94*(1), 47–57.

Klotz, J. M., & Rosenberg, R. M. (1991). Chemical thermodynamics. *Basic theory and methods* (pp. 439–443). Malabar, Florida: Krieger.

Lancia, A., Musmarra, D., & Pepe, F. (1997). Modeling of SO_2 Absorption into limestone suspensions. *Industrial & Engineering and Chemical Research*, *36*, 197–203.

Lancia, A., Musmarra, D., Pepe, F., & Volpicelli, G. (1994). SO_2 absorption in A bubbling reactor using limestone suspensions. *Chemical Engineering Science*, *49*(24A), 4523–4532.

Lowell, P. S., Ottmers, D. M., Schwitzgebel, K., Strange, T. I., & Deberry, G. W. (1970). A theoretical description of the limestone injection-wet scrubbing process. PB 193-029. In *US Environmental Protection Agency*, Vol. I (pp. 60–78). CPA-22-69-138. Radian Corporation, Austin, Texas.

Olausson, S., Wallin, M., & Bjerle, I. (1993). A model for the absorption of sulfur dioxide into a limestone slurry. *Chemical Engineering Journal*, *51*, 99–108.

Pasiuk-Bronikowska, W., & Rudzinski, K. J. (1991). Absorption of SO_2 into aqueous systems. *Chemical Engineering Science*, *46*(9), 2281–2291.

Pasiuk-Bronikowska, W., & Ziajka, J. (1985). Oxygen absorption in aqueous sulphur dioxide solutions. *Chemical Engineering Science*, *40*(8), 1567–1572.

Pasiuk-Bronikowska, W., Ziajka, J., & Bronikowski, T. (1992). *Autoxidation of sulphur compounds*. Warsaw, Poland: E. Horwood & PWN-Polish Scientific Publishers.

Reid, R., Prausnitz, J. M., & Sherwood, T. K. (1987). *The properties of gases and liquids*. Third Edition. London: McGraw–Hill.

Sada, E., Kumazawa, H., Hashizume, I., & Nishimura, H. (1982). Absorption of dilute SO_2 into aqueous slurries of $CaSO_3$. *Chemical Engineering Science*, *37*, 1432–1435.

Sada, E., Kumazawa, H., & Lee, C. H. (1984). Absorptions of carbon dioxide and sulfur dioxide into aqueous concentrated slurries of calcium hydroxide. *Chemical Engineering Science*, *39*(1), 117–120.

Tseng, P. C., & Rochelle, G. (1986). Dissolution rate of calcium sulfite hemihydrate in flue gas desulfurization processes. *Environmental Progress*, *5*(1), 34–40.

Uchida, S., & Ariga, O. (1985). Absorption of sulfur dioxide into limestone slurry in a stirred tank. *Canadian Journal of Chemical Engineering*, *63*(5), 778–783.

Uchida, S., Moriguchi, H., Maejima, H., Koide, K., & Kageyama, S. (1978). Absorption of sulfur dioxide into limestone slurry in a stirred tank reactor. *Canadian Journal of Chemical Engineering*, *56*, 690–697.

Ulrich, R. K., Rochelle, G. T., & Prada, R. E. (1986). Enhanced oxygen absorption into bisulphite solutions containing transition metal ion catalysts. *Chemical Engineering Science*, *41*(8), 2183–2191.

Versteeg, G. F., Blauwhoff, P. M. M., & van Swaaij, W. P. M. (1987). The effect of diffusivity on gas–liquid mass transfer in stirred vessels. Experiments at atmospheric and elevated pressures. *Chemical Engineering Science*, *42*(5), 1103–1119.